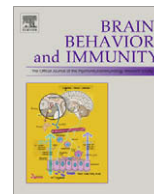




Contents lists available at ScienceDirect

Brain, Behavior, and Immunity

journal homepage: www.elsevier.com/locate/ybrbi

Bid mediates fission, membrane permeabilization and peri-nuclear accumulation of mitochondria as a prerequisite for oxidative neuronal cell death

Julia Grohm^a, Nikolaus Plesnila^b, Carsten Culmsee^{a,*}

^a Institut für Pharmakologie und Klinische Pharmazie, Fachbereich Pharmazie, Philipps-Universität Marburg, Karl-von-Frisch Straße 1, 35043 Marburg, Germany

^b Department of Physiology, Royal College of Surgeons in Ireland (RCSI), 123 St. Stephen's Green, Dublin 2, Ireland

ARTICLE INFO

Article history:

Received 20 September 2009

Received in revised form 27 November 2009

Accepted 27 November 2009

Available online xxxx

Keywords:

Neurodegeneration

Neuronal cell death

Glutamate

Oxidative stress

Mitochondria

Fission and fusion

Bid

Apoptosis inducing factor

Mitochondrial fission

Mitochondrial membrane potential

Apoptosis

Bcl-2

ABSTRACT

Mitochondria are highly dynamic organelles that undergo permanent fusion and fission, a process that is important for mitochondrial function and cellular survival. Emerging evidence suggests that oxidative stress disturbs mitochondrial morphology dynamics, resulting in detrimental mitochondrial fragmentation. In particular, such fatal mitochondrial fission has been detected in neurons exposed to oxidative stress, suggesting mitochondrial dynamics as a key feature in intrinsic death pathways. However, the regulation of mitochondrial fission in neurons exposed to lethal stress is largely unknown. Here, we used a model of glutamate toxicity in HT-22 cells for investigating mitochondrial fission and fusion in neurons exposed to oxidative stress. In these immortalized hippocampal neurons, glutamate induces glutathione depletion and increased formation of reactive oxygen species (ROS). Glutamate toxicity resulted in mitochondrial fragmentation and peri-nuclear accumulation of the organelles. Further, mitochondrial fission was associated with loss of mitochondrial outer membrane potential (MOMP). The Bid-inhibitor BI-6c9 prevented MOMP and mitochondrial fission, and protected the cells from cell death. In conclusion, oxidative stress induced by glutamate causes mitochondrial translocation of Bid thereby inducing mitochondrial fission and associated mitochondrial cell death pathways. Inhibiting regulators of pathological mitochondrial fragmentation is proposed as an efficient strategy of neuroprotection.

© 2009 Elsevier Inc. All rights reserved.

1. Introduction

In neurons, mitochondrial function and energy supply is a prerequisite for the function of ion channels, transport proteins, release and recycling of neurotransmitters, calcium buffering, and regulation of apoptosis (Chipuk and Green, 2008; Green, 2005; Kluck et al., 1997; Knott and Bossy-Wetzel, 2008). Mitochondria form a highly dynamic tubular network, and the shape and the size of these organelles are regulated by movements along the cytoskeleton and by frequented fusion and fission events (Bereiter-Hahn and Voth, 1994; Parone et al., 2008; Rube and van der Bliek, 2004). In neurons, such morphological dynamics facilitate the redistribution of mitochondria in response to local changes in the demand for ATP, for example in active synapses or dendrites. Moreover, mitochondrial fission is essential for calcium regulation (Cheung et al., 2007). On the other hand, mitochondrial fusion is needed to exchange mtDNA and other mitochondrial components that may become damaged over time (Okamoto and Shaw, 2005; Chan, 2006; Santel and Frank, 2008). Mitochondrial fusion is there-

fore important for mitochondrial regeneration and proper function. The rates of fission and fusion are usually balanced but vary between different cell types and may also respond to environmental changes and cellular stress.

Mitochondrial morphology dynamics are controlled by the opposing actions of different dynamin protein family members that are located at or within mitochondria. While many molecules comprising the fission machinery have been identified in yeast, only three mammalian orthologues have been found so far: fission 1 (Fis1), dynamin-related protein 1 (Drp-1), and Endophilin B1 are known to be required for mitochondrial fission in mammals (Karbowski et al., 2004). The mechanisms by which cytosolic Drp-1 becomes activated and recruited to the mitochondria to interact with Fis1 thereby inducing mitochondrial fission, however, remain unclear (Cheung et al., 2007). In contrast to fission, mitochondrial fusion requires both outer and inner mitochondrial components, such as Mitofusin 1 and 2 (Mfn1, 2) and Optical Atrophy protein 1 (Opa1).

Mutations of Mfn2 and Opa1 are associated with severe disturbances in mitochondrial dynamics and hereditary neuropathies, such as Charcot-Marie Tooth disease and autosomal dominant optic atrophy, respectively (Liesa et al., 2009).

* Corresponding author. Fax: +49 6421 28 25720.

E-mail address: culmsee@staff.uni-marburg.de (C. Culmsee).

Increasing evidence now also suggests that disturbance of mitochondrial dynamics contribute to neuronal dysfunction and death in various neurodegenerative diseases. For example, rates of mitochondrial fission are significantly accelerated when Cytochrome C is released from mitochondria during apoptosis (Desagher and Martinou, 2000; Wasilewski and Scorrano, 2009) or when mitochondria are depolarized with ionophores (Ishihara et al., 2003). Both, fission and fusion defects may limit mitochondrial motility, decrease energy production, promote oxidative stress and mtDNA deletion, and impair Ca^{2+} buffering, thereby contributing to intrinsic death pathways (Knott and Bossy-Wetzel, 2008; Bossy-Wetzel et al., 2003; Lackner and Nunnari, 2008). Mitochondrial fragmentation in neurodegenerative processes may result from increased mitochondrial fission, decreased mitochondrial fusion, or both.

It has been established that pro-apoptotic Bcl-2 protein family members such as Bax, Bak and Bid mediate mitochondrial dysfunction and associated death signaling in neurons (Arnoult, 2007; Darnal and Korsmeyer, 2004; Wang, 2001; Culmsee and Plesnila, 2006), and a number of recent findings suggested that such intrinsic death pathways are associated with extensive mitochondrial fragmentation (Bossy-Wetzel et al., 2003; Karbowski and Youle, 2003; Wang, 2001; Youle and Karbowski, 2005). In the present study, we addressed mitochondrial morphology dynamics in a model of glutamate-induced neurotoxicity in HT-22 cells aiming to elucidate whether Bid was involved in the regulation of mitochondrial dynamics and associated mitochondrial cell death pathways after induction of oxidative stress.

2. Experimental procedures

2.1. Cell culture and induction of neuronal cell death

HT-22 cells were cultured in Dulbecco's modified Eagle medium (DMEM, Invitrogen, Karlsruhe, Germany) supplemented with 10% heat-inactivated fetal calf serum, 100 U/ml penicillin, 100 µg/ml streptomycin and 2 mM glutamine (PAA Laboratories GmbH, Germany). Glutamate (1–5 mM) was added to the serum containing medium and cell viability was evaluated 18 h later.

2.2. Plasmids and gene transfer

The pIRES-tBid vector, mGFP vector and control vectors were generated as described previously (Kazhdan et al., 2006; Duvezin-Caubet et al., 2006). For plasmid transfections 7×10^4 HT-22 neurons were seeded in 24-well plates. Antibiotic containing growth medium was removed and replaced with 900 µl antibiotic free growth medium. Lipofectamine 2000 (Invitrogen, Karlsruhe, Germany) mGFP, pIRES-tBid plasmide or empty vector pcDNA 3.1+ were dissolved separately in Optimem I (Invitrogen, Karlsruhe, Germany). After 10 min of equilibration at room temperature each DNA solution was combined with the respective volume of the Lipofectamine solution, mixed gently, and allowed to form plasmid liposomes for further 20 min at room temperature. The transfection mixture was added to the antibiotic-free cell culture medium to a final concentration of 1 µg DNA, and 1.5 µl/ml Lipofectamine 2000 in HT-22 neurons. Controls were treated with 100 µl/ml Optimem I only, and vehicle controls with 1.5 µl/ml Lipofectamine 2000.

2.3. Immunostaining and confocal laser scanning, fluorescence microscopy

For detection of mitochondrial morphology changes during cell death, HT-22 neurons were transfected with the mGFP plasmid, respectively. Twenty-four hours after transfection HT-22 cells were

seeded in collagen A-coated Ibitreat µ-slide 8-well plates (Ibidi, Munich, Germany) at a density of 1.7×10^4 /well for endpoint analysis on a fluorescence microscope (DMI6000, Leica, Germany).

Alternatively, mitochondria were visualized by MitoTracker Green/Red according to the manufacturer's protocol (Invitrogen, Karlsruhe, Germany). Endpoint pictures were taken after fixation with 4% PFA and DAPI counterstaining of the nuclei 18 h after onset of treatment. Images were acquired using a fluorescence microscope (DMI6000, Leica, Germany) and a confocal laser scanning microscope (LSM 510, Carl Zeiss, Jena, Germany) equipped with an UV, an argon, and a Helium/Neon laser delivering light at 364, 488, and 543 nm, respectively. Light was collected through a 40×1.3 NA, 63×1.4 NA, or 100×1.3 NA oil immersion objectives. DAPI fluorescence was excited at 364 nm and emission was achieved by using the 385 nm long pass filter. Mitotracker Green and mGFP were excited at 488 nm and 543 nm and emissions were detected using 505–530 nm band pass (green) and 560 nm long pass filters (red), respectively.

2.4. Evaluation of mitochondrial morphology

HT-22 cells were transfected with mGFP as described before. After 24 h the cells were reseeded on collagen A-coated Ibitreat µ-slide 8-well plates (Ibidi, Munich, Germany) and treated for 18 h. Endpoint pictures were taken after fixation with 4% PFA and DAPI counterstaining of the nuclei 18 h after onset of treatment. Counting of four different types of mitochondrial states was done in at least four independent experiments with 500 cells. From at least 6 independent pictures per experiment, mitochondrial length was calculated by Image J software (NIH, Bethesda, USA).

2.5. Evaluation cell viability and apoptosis

For morphological analysis of cell viability, transmission light microscopy of living HT-22 neurons growing as monolayers was performed using an Axiovert 200 microscope (Carl Zeiss, Jena, Germany) equipped with a Lumenera Infinity 2 digital camera (Lumenera Corporation, Ottawa, Canada). Light was collected through a 10×2.5 NA objective (Carl Zeiss, Jena, Germany), and images were captured using phase contrast. Digital image recording and image analysis were performed with the INFINITY ANALYZE software (Lumenera Corporation, Ottawa, Canada). Quantification of cell viability in HT-22 cells was performed in 96-well plates by 3-(4,5-dimethylthiazol-2-yl)-2,5-diphenyltetrazolium bromide (MTT) reduction at 0.25 mg/ml for 2 h (Liu et al., 1997). The reaction was terminated by adding dimethylsulfoxide after freezing the plate without media at -80°C for at least 1 h and absorbance was then determined at 590 nm versus 630 nm (Fluostar OPTIMA, BMG Labtech, Offenburg, Germany). Apoptotic cell death was detected by annexin-V/propidium iodide staining and subsequent flow cytometry analysis. Cells were harvested 18 h after glutamate-treatment by using Trypsin/EDTA, washed once in PBS and stained according to the manufacturer's protocol (Annexin V-FITC Detection Kit, PromoKine, Promocell, Germany). Apoptotic and necrotic cells were determined using FACSScan (BD Bioscience, Germany). Annexin V-FITC was excited at 488 nm and emission was detected through a 530 ± 40 nm band pass filter. Propidium iodide was excited at 488 nm and fluorescence emission was detected using a 680 ± 30 nm band pass filter. To exclude cell debris and doublets, cells were appropriately gated by forward versus side scatter and pulse width, and 1×10^4 gated events per sample were collected. Surviving cells did not show any staining whereas annexin V staining indicated apoptosis and cells positive for both annexin V and propidium iodide were regarded necrotic.

2.6. Detection of oxidative stress

Intracellular reactive oxygen species (ROS) were detected by dichlorodihydrofluorescein-diacetate (DCF). Within 6–17 h after glutamate treatment HT-22 cells were loaded with 1 μ M CM-H2DCFDA (Invitrogen, Karlsruhe, Germany) for 30 min and fluorescence at 530 nm was monitored using a CyanTM MLE flow cytometer (DakoCytomation, Copenhagen, Denmark) at an excitation wavelength of 488 nm. For detection of cellular lipid peroxidation cells were loaded with 2 μ M BODIPY 581/591 C11 for 60 min in standard medium 6–17 h after glutamate treatment. Cells were then collected, washed and resuspended in phosphate-buffered saline (PBS) and flow cytometry was performed using 488 nm UV line argon laser for excitation and BODIPY emission was recorded on channels FL1 at 530 nm (green) and FL2 at 585 nm (red). Data were collected from at least 20,000 cells.

2.7. Analysis of mitochondrial membrane potential

Mitochondrial membrane potential of HT-22 neurons was determined by 5,5',6,6'-tetrachloro-1,1',3,3'-tetraethylbenzimidazolylcarbocyanine iodide (JC-1) reduction. HT-22 neurons were stained with JC-1 (Mitoprobe, Invitrogen, Karlsruhe, Germany) according to the manufacturer's protocol and analyzed by subsequent flow cytometry or epifluorescence microscopy. After glutamate treatment (12 h), JC-1 was added to each well of the different treatment conditions to a final concentration of 2 μ M. Living-control cells received vehicle (DMSO, 0.1% final concentration) and damage-control cells were treated with carbonyl cyanide m-chlorophenylhydrazone (CCCP) 5 min before staining to induce mitochondrial membrane depolarization. Detached cells in the medium were collected and combined with the attached cells harvested with standard Trypsin/EDTA (TE, Biochrom, Berlin, Germany) in PBS. Trypsin incubation was stopped by adding 800 μ l serum containing medium to each well. Cells were centrifuged at 170g, washed once with PBS, and kept in 700 μ l PBS on ice until analysis of JC-1 fluorescence using a FACscan (BD Bioscience, Germany). JC-1 green fluorescence indicating uptake of the dye was excited at 488 nm and emission was detected using a 530 \pm 40 nm band pass filter. JC-1 red fluorescence indicating intact mitochondrial membrane potential was excited at 488 nm and emission was detected using a 613 \pm 20 nm band pass filter. To exclude cell debris and doublets, cells were appropriately gated by forward versus side scatter and pulse width, and 1 \times 10⁴ gated events per sample were collected from 3 to 4 independent samples per treatment condition.

2.8. Real-time measurements with xCELLigence System

The xCELLigence System (Roche, Penzberg, Germany) monitors cellular events in real time by measuring the electrical impedance between micro-electrodes integrated into the bottom of custom made tissue culture plates (E-Plates). Since cells have a very high electrical resistance, the more cells are attached to the bottom of the E-Plates, the higher the electrical impedance will be. Thus, the electrical impedance, which is displayed as Normalized Cell Index (NCI), can be used to monitor cell viability, number, morphology, and adhesion in a large number of tissue culture wells simultaneously, at any given frequency, and over any desired period of time without removing the plates from the incubator. HT-22 cells were seeded in a density of 4500 cells/well in 96-well E-plates (Roche, Penzberg, Germany). Twenty-four hours after seeding cells were incubated with vehicle, BI-6c9 (10 μ M) (Sigma-Aldrich, Germany), glutamate (3 mM and 5 mM), or glutamate + BI-6c9 (10 μ M).

2.9. Statistical analysis

All data are given as means \pm standard deviation (SD). Statistical multiple comparisons were performed by analysis of variance (ANOVA) followed by Scheffé's post hoc test. Calculations were performed with the Winstat standard statistical software package (R. Fitch Software, Bad Krozingen, Germany).

3. Results

3.1. Classification of mitochondrial morphology

Four categories of mitochondrial morphology were defined for the quantification of mitochondrial fission in HT22 cells (Fig. 1A). Healthy cells have Category 1 (I) mitochondria that form a tubular network. These mitochondria are equally distributed throughout the cytosol. Category 2 (II) mitochondria appear shorter than Category 1 mitochondria but are still forming long tubules. Cells containing large round mitochondria distributed throughout the cytosol are defined as Category 3 (III). These cells are still alive and do not show apoptotic features, e.g. shrunken nuclei, and do not detach from the well. In contrast, damaged and dying cells show small rounded mitochondria of different sizes that are located close to the nucleus. These mitochondria are defined as Category 4 (IV). To quantify mitochondrial morphology, cells were transfected with mGFP as described before and used for experiments 24 h after they were seeded out in 8-well ibidi slides. Mitochondrial categorization was performed in 500 cells per well by an investigator blinded towards the treatment of the cells. Mitochondrial length was quantified semi-automatically by using the Image J image analysis software (Fig. 1B).

3.2. Oxidative stress resulted in pronounced mitochondrial fragmentation

Exposure of HT-22 neurons to glutamate resulted in enhanced ROS formation in a time-dependent manner (Fig. 2A). ROS formation was associated with a significant change in mitochondrial morphology. Mitochondria were organized as a tubular network under control conditions, however, after exposure to glutamate the network broke up in short tubules and round fragments (Fig. 2B). These changes resulted in a significant shortage of mitochondrial length (Fig. 2C) and in an evident shift of mitochondria from Category 1 or 2 into Categories 3 and 4 (Fig. 2D). These changes, which are well in line with the definition of mitochondrial fission, were associated with a decrease of cell viability from 100% to 20% (Fig. 4A).

3.3. Bid as a mediator of glutamate-induced mitochondrial fission

Translocation of the pro-apoptotic Bcl-2 family member Bid to mitochondria results in AIF translocation to the nucleus and cell death, as previously evaluated in cells expressing Bid-red fusion protein and AIF-GFP (Landshamer et al., 2008). In the current experiments the highly specific Bid-inhibitor BI-6c9 prevented the fission of mitochondria in glutamate-exposed HT-22 cells and the shift of mitochondrial morphology from a tubular, network-like structure (Categories 1 and 2) to a small, round shape (Categories 3 and 4) and restored mitochondrial morphology to almost normal levels (Fig. 3A and B). The preservation of mitochondrial morphology by BI-6c9 was associated with a normalization of mitochondrial membrane potential (Fig. 3C and D) suggesting that mitochondrial morphology is closely linked to mitochondrial function and that ROS-induced mitochondrial damage and loss of function are not the result of unspecific membrane damage, but of

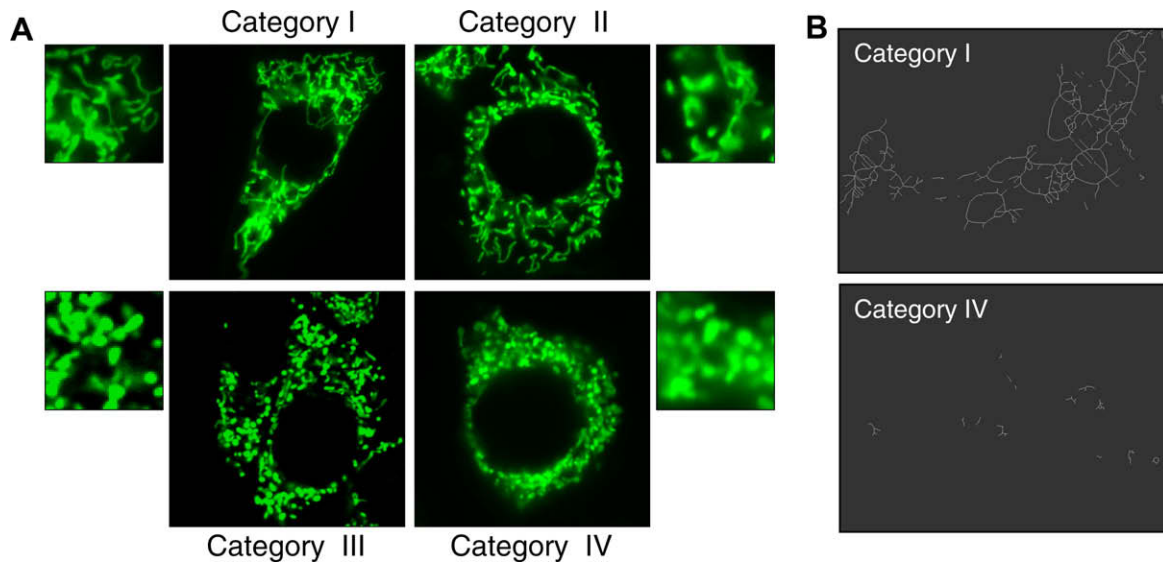


Fig. 1. (A) Classification of different morphology categories of mitochondria in HT-22 cells. Category I: elongated, Category II: tubule-like, Category III: intermediate, Category IV: fragmented. Magnifications for each category show mitochondrial morphology for each category in detail. (B) Photomicrographs analyzed mitochondria of Categories I and IV by Image J.

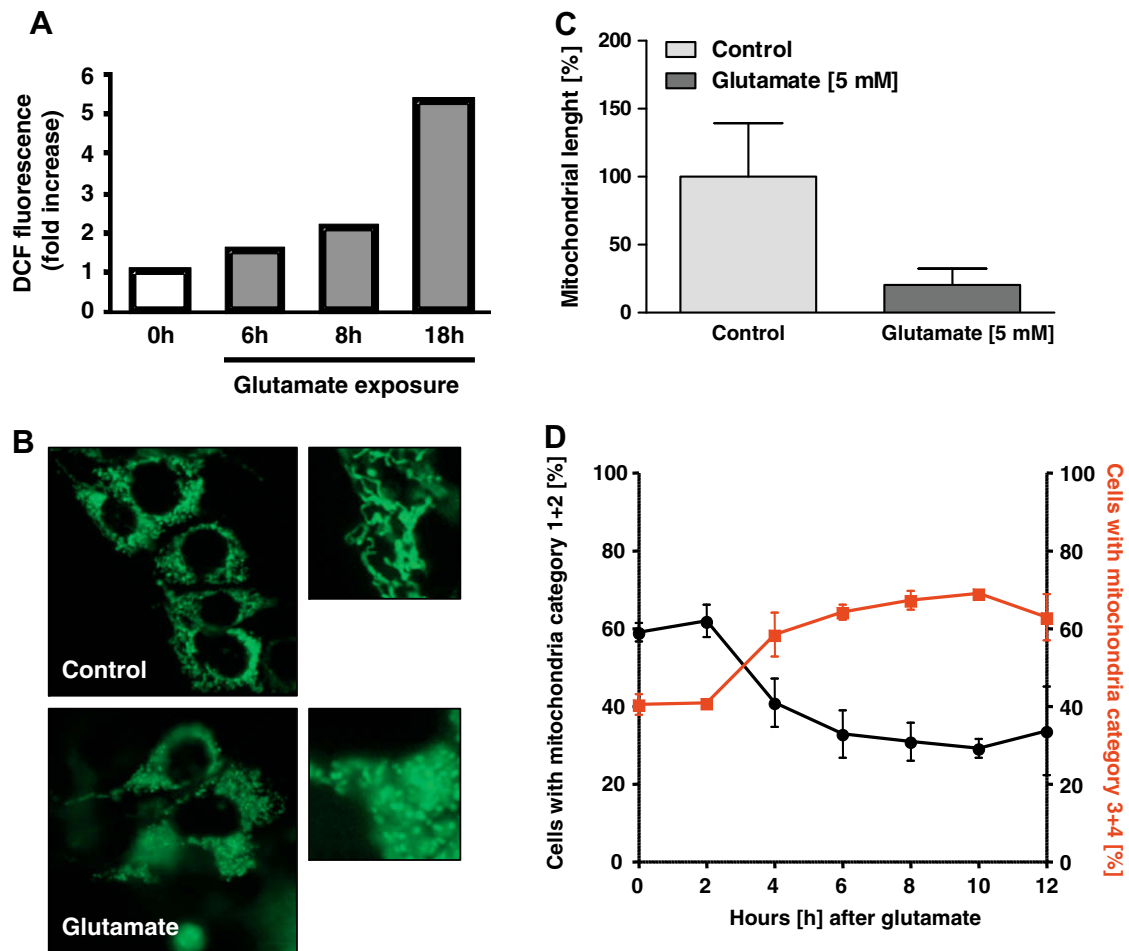


Fig. 2. Oxidative stress induces pronounced fragmentation of mitochondria in HT-22 neurons. (A) Increase in ROS formation 18 h after glutamate treatment. (B) Photomicrographs show changes of mitochondrial morphology in HT-22 cells transfected with mitochondria-targeted GFP (mGFP) and treated with glutamate (5 mM) for 18 h. (C) Mitochondrial length measurements in glutamate-treated HT-22 cells. (D) Time-dependent shifting of mitochondria Categories I and II over 12 h to mitochondria Categories III and IV in culture of HT-22 neurons.

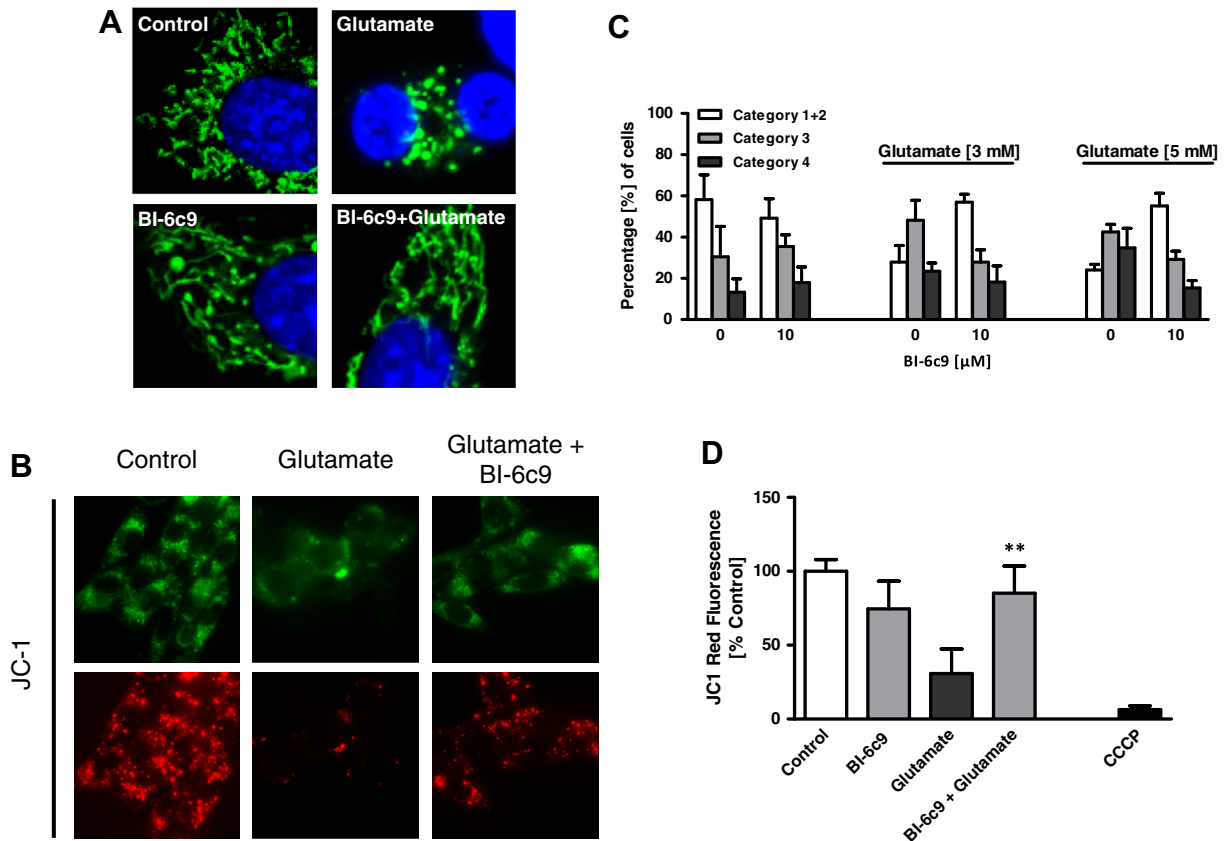


Fig. 3. Bid-inhibitor BI-6c9 prevents Bid translocation to mitochondria, mitochondrial fission and glutamate-induced mitochondrial depolarization. (A) Fluorescence photomicrographs show that Bid-inhibitor BI-6c9 (10 μ M) prevented the fission of mitochondria in glutamate-exposed (5 mM, 18 h) HT-22 cells. (B) Mitochondrial membrane potential was analyzed by JC-1 fluorescence: upper panels show epifluorescence photomicrographs indicating equal cellular uptake of JC-1 by green fluorescence, lower panels depict intact mitochondria exposing red fluorescence. Glutamate-treated (5 mM, 12 h) HT-22 cells show significantly reduced red fluorescence compared to controls whereas BI-6c9 (10 μ M) prevents the breakdown of the mitochondrial membrane potential as indicated by preservation of the red JC-1 fluorescence. (C) Quantification of mitochondrial morphology: Category 1 + 2: elongated, tubule-like, Category 3: intermediate, Category 4: fragmented. *** p < 0.001 compared to glutamate 3 mM/5 mM and BI-6c9-treated cells (ANOVA, Scheffé's). (D) FACS analyses of $n = 3$ independent experiments per group reveal a decrease of the red JC-1 fluorescence to 30 % of control levels 12 h after glutamate treatment (5 mM) which is prevented by BI-6c9. Glutamate treatment was as effective as the positive damage-control CCCP which causes a fast breakdown of the mitochondrial membrane potential. ** p < 0.01 compared to controls and BI-6c9-treated cells (ANOVA, Scheffé's).

specific, Bid-mediated cell death signaling. The Bid-inhibitor prevented glutamate-induced breakdown of the mitochondrial membrane potential in HT-22 neurons (Fig. 3C and D) indicating that activation and mitochondrial translocation of Bid was a key event for the glutamate-induced loss of mitochondrial integrity and function.

3.4. Restoration of mitochondrial morphology and function – effect on cell viability

Inhibition of Bid did not only result in the preservation of mitochondrial morphology and function but also preserved cell viability in glutamate-treated HT-22 cells as demonstrated by the MTT assay and the novel xCELLigence System (Fig. 4). While exposure to glutamate resulted in a reduction of cell viability from 100% to 20%, inhibition of Bid by BI-6c9 restored cell viability to almost baseline levels (Fig. 4A). The protective effect of Bid inhibition could be confirmed by the real-time analysis of the electrical impedance using the xCELLigence System (Fig. 4B). Treatment of HT-22 cells with glutamate at concentrations of 3 mM and 5 mM resulted in an immediate decrease of the Normalized Cell Index (NCI) as result of the dilution of the cell culture medium by the glutamate solution. The NCI normalized on the point in time of glutamate addition in all control and treatment groups, however, only in the glutamate-treated cell the NCI stated to decrease again

between 7 and 5.5 h later, indicating progressive cell death (Fig. 4B, ¹blue and pink graphs, glutamate 3, 5 mM). It is interesting to note that, once started, the loss of cellular impedance was observed within a relatively small and constant time window of 2–3 h, suggesting that cell death and detaching of the cells occurred rapidly and in a highly synchronized manner. Inhibition of Bid by BI-6c9 resulted in a complete protection of this delayed, glutamate-induced loss of the NCI and, hence, in a prevention of cell death as also confirmed by the MTT assay. These data indicate that glutamate-induced ROS production induces specific, Bid-mediated cell death signaling which results in a delayed loss of mitochondrial morphology and function and cell death.

4. Discussion

The present study provides evidence for a key role of Bid in mitochondrial pathways of neuronal apoptosis caused by oxidative stress. Our data suggest that glutamate significantly disturbed the delicate balance between mitochondrial fission and fusion in neuronal cells and that fission of mitochondria accompanies cell death. The molecular key regulators and mechanisms of mitochondrial fission and fusion are largely unknown, in particular in the context

¹ For interpretation of color in Fig. 4, the reader is referred to the web version of this article.

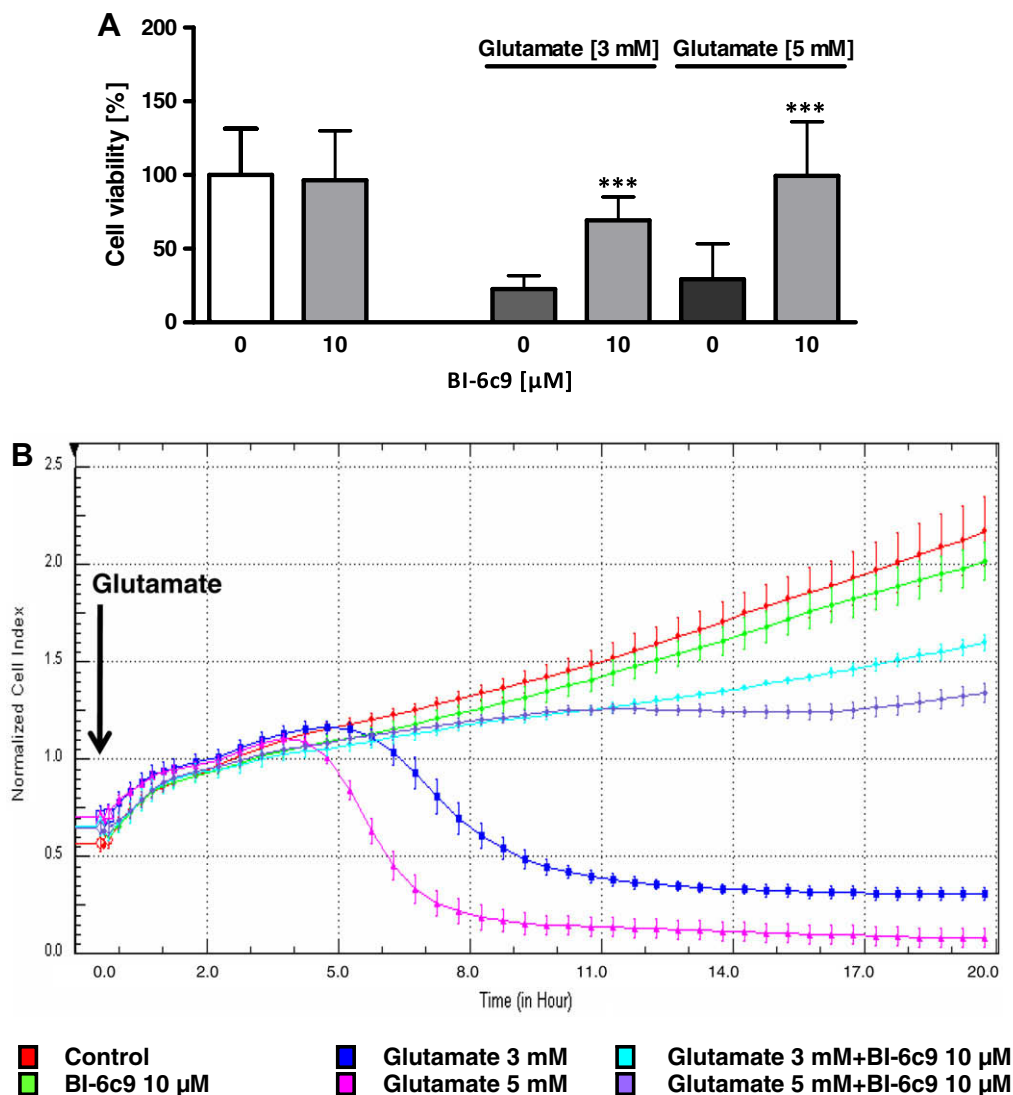


Fig. 4. Real-time detection of cellular impedance for detection of cellular viability. (A) MTT assay was used to determine the cell viability 18 h after glutamate treatment. BI-6c9 attenuated glutamate-induced cell death. (B) Real-time detection of cellular impedance was done with xCELLigence System (Roche, Penzberg, Germany). Normalized Cell Index (NCI) of HT-22 cells shows reduction of cell viability around 4.5 h after glutamate treatment. BI-6c9 significantly attenuated the loss of cell viability after glutamate excitotoxicity. HT-22 cells were cultured for 48 h in E-plates and treated with 3 mM and 5 mM glutamate and BI-6c9 (10 μ M) for 18 h.

of apoptosis signaling. In the currently used model system, glutamate induces cell death through glutathione depletion and accelerated formation of reactive oxygen species (ROS) (Seiler et al., 2008). As previously demonstrated glutamate-induced oxidative neuronal cell death is associated with translocation of Bid to mitochondria and the release of mitochondrial AIF to the nucleus (Culmsee et al., 2005b; Landshamer et al., 2008). In the present study, we demonstrate that these mitochondrial pathways of apoptosis are associated with enhanced mitochondrial fission and relocation of fragmented mitochondria to the nucleus. Such mitochondrial fragmentation and the associated loss of the mitochondrial membrane potential were prevented by BI-6c9, a highly specific Bid inhibitor, indicating a major role of Bid in death signaling upstream of mitochondrial fission, and the altered cellular distribution and integrity of these organelles in neuronal cells.

Mitochondria-dependent apoptosis is highly regulated by a series of pro- and anti-apoptotic proteins of the Bcl-2 family which control, among others, permeabilization of the mitochondrial outer membrane (Kroemer et al., 2007; Youle and Strasser, 2008). Mitochondrial membrane permeabilization is believed to result from Bcl-2 protein conformation changes, protein–protein and protein–

membrane-interactions that are initiated by binding of tBid to the mitochondrial membrane and interaction of tBid with Bax. Subsequent Bax oligomerization and Bax/Bak interactions lead to mitochondrial membrane permeabilization. Under physiological conditions Bcl-XL inhibits this process by binding to and sequestering membrane-bound tBid (Billen et al., 2008; Lovell et al., 2008). It was shown that Bax/Bak complexes promote fusion of mitochondria in healthy cells but also participate in mitochondrial fission during apoptosis (Brooks and Dong, 2007). Both, Bax and Bak undergo changes in submitochondrial localization and alterations of conformation during apoptosis, which likely alters their interaction with proteins such as Mitofusin (Mfn2) and Endophilin B1 and, consequently, involves these pro-apoptotic Bcl-2 family proteins in the regulation of the mitochondrial morphology (Suen et al., 2008). Mitochondrial fission is mainly mediated by dynamin-related protein 1 (Drp-1), a large soluble GTPase. Most Drp-1 is found in the cytosol from where it can shuttle to mitochondria to interact with Bax and Mfn 2 (Wasiak et al., 2007). Additional proteins, like Fis1 or endophilin B1, act downstream of Drp1 and further post-translational modifications of Drp-1 including ubiquitination, sumoylation, and phosphorylation play regulatory roles in Drp-1

function and mitochondrial division (Knott et al., 2008; Lackner and Nunnari, 2008). In the present study we found that glutamate toxicity was associated with significantly enhanced mitochondrial fragmentation, suggesting that the mitochondrial fission machinery was involved in the detrimental signaling pathways that execute glutamate-induced cell death, and these mechanisms required the activation and mitochondrial translocation of the pro-apoptotic Bcl-2 protein Bid. The precise mechanism of Bid-dependent mitochondrial fragmentation, loss of mitochondrial membrane potential and release of pro-apoptotic mitochondrial proteins may involve interactions of Bid with Bax and Bak, and with other factors of the fission and fusion machinery.

The results presented here further confirmed that depolarization of the mitochondrial outer membrane is an important key event of mitochondrial apoptosis induced by oxidative stress. Glutamate-induced mitochondrial fission in HT-22 neurons was associated with depolarization of the mitochondrial membrane, and both events were apparently Bid dependent. Pharmacological inhibition of Bid prevented mitochondrial outer membrane depolarization, and this rescue of mitochondrial membrane integrity was associated with preserved mitochondrial morphology and enhanced neuronal survival. As shown previously, the Bid-inhibitor BI-6c9 also prevented mitochondrial Bid translocation and protected the cells from mitochondrial AIF release and caspase-independent cell death in neurons (Landshamer et al., 2008). In addition, similar protective effects on mitochondrial integrity and reduced ROS formation were obtained in the present model of glutamate toxicity using Bid siRNA. These findings support the conclusion that Bid activation and subsequent mitochondrial translocation are early key events recruiting mitochondria to the death machinery in neurodegenerative pathologies associated with glutamate toxicity and oxidative stress.

In this context it is interesting to note that such recruitment of the mitochondria was literally detectable by the accumulation and agglomeration of the highly fragmented mitochondria in the vicinity of the nucleus, suggesting that in dying neurons enhanced mitochondrial fission was permissive for an enhanced transport of these organelles towards the nucleus. This phenomenon of mitochondrial kinetics fits well with the kinetics of cell death execution that has been established in the present model of glutamate-induced oxidative cell death. In particular, multiple lines of evidence proposed a prelude of several hours for the glutamate-induced glutathione depletion and Bid-mediated disruption of mitochondrial function. In previous studies we could define a therapeutic time window of 8–10 h after the onset of the glutamate challenge that allowed delayed application of antioxidants or the Bid-inhibitor to rescue mitochondrial function and to prevent neural cell death (Landshamer et al., 2008 and data not shown). Here, we confirmed this time window by real-time analysis of cell death using continuous measurements of cellular impedance. These impedance measurements correlated very well with established measurements of cell viability by the standard MTT assay and clearly demonstrated that oxidative cell death occurred not before 8–10 h after onset of the glutamate challenge. In this time frame, enhanced mitochondrial fission and peri-nuclear accumulation of the organelles precedes the final execution of cell death that is featured by mitochondrial membrane permeabilization and release of mitochondrial AIF to the nucleus. Further, the observed agglomeration of fragmented mitochondria in close vicinity to the nucleus further explains the relatively fast kinetics of the following death execution that occurs within 1–2 h after the precluding events and involves rapid translocation of AIF to the nucleus as shown by video-microscopy in our earlier work (Landshamer et al., 2008). The high number of fragmented and permeabilized mitochondria is likely to be a prerequisite for the observed rapid transfer of the deadly mitochondrial protein over the short distance to the nuclei

of lethally stressed cells. In conclusion, enhanced mitochondrial fission is a key feature for programmed cell death execution, since fragmented mitochondria can easily accumulate around the nucleus where they release their deadly message after reaching the point of no return marked by mitochondrial membrane permeabilization.

Our results demonstrate a pivotal role for Bid upstream of such mitochondrial dysfunction in neurons exposed to oxidative stress. This conclusion is confirmed by experiments demonstrating pronounced neuroprotective effects of the Bid-inhibitor BI-6c9 in models of glutamate-induced excitotoxicity and oxygen–glucose deprivation in primary cultured neurons, and similar studies in HT22 neurons using Bid siRNA (Becattini et al., 2006; Culmsee et al., 2005a; Landshamer et al., 2008). Further, genetic deletion of Bid attenuated neuronal death in a model of oxygen–glucose deprivation *in vitro* and reduced brain damage in models of cerebral ischemia and brain trauma *in vivo* (Bermppohl et al., 2007; Plesnila et al., 2001).

Overall, Bid is a key regulator of mitochondrial neuronal cell death pathways associated with enhanced oxidative stress. Bid-mediated neuronal cell death involves mitochondrial fission, mitochondrial membrane permeabilization, and release of mitochondrial cell death regulators such as AIF. Here, we demonstrate for the first time that Bid is a key regulator of mitochondrial fission, mitochondrial relocation to the nucleus, and mitochondrial integrity in neuronal cells exposed to oxidative stress. Therefore, Bid is a promising therapeutic target to prevent mitochondrial fragmentation and dysfunction which are hallmarks of neuronal cell death in most neurodegenerative diseases.

References

- Arnoult, D., 2007. Mitochondrial fragmentation in apoptosis. *Trends Cell Biol.* 17, 6–12.
- Becattini, B., Culmsee, C., Leone, M., Zhai, D.Y., Zhang, X.Y., Crowell, K.J., Rega, M.F., Landshamer, S., Reed, J.C., Plesnila, N., Pellecchia, M., 2006. Structure–activity relationships by interligand NOE-based design and synthesis of antiapoptotic compounds targeting Bid. *Proc. Natl. Acad. Sci. USA* 103, 12602–12606.
- Bereiter-Hahn, J., Voth, M., 1994. Dynamics of mitochondria in living cells: shape changes, dislocations, fusion, and fission of mitochondria. *Microsc. Res. Tech.* 27, 198–219.
- Bermppohl, D., You, Z., Lo, E.H., Kim, H.H., Whalen, M.J., 2007. TNF alpha and Fas mediate tissue damage and functional outcome after traumatic brain injury in mice. *J. Cereb. Blood Flow Metab.* 27, 1806–1818.
- Billen, L.P., Kokoski, C.L., Lovell, J.F., Leber, B., Andrews, D.W., 2008. Bcl-XL inhibits membrane permeabilization by competing with Bax. *PLoS Biol.* 6, e147.
- Bossy-Wetzel, E., Barsoum, M.J., Godzik, A., Schwarzenbacher, R., Lipton, S.A., 2003. Mitochondrial fission in apoptosis, neurodegeneration and aging. *Curr. Opin. Cell Biol.* 15, 706–716.
- Brooks, C., Dong, Z., 2007. Regulation of mitochondrial morphological dynamics during apoptosis by Bcl-2 family proteins: a key in Bak? *Cell Cycle* 6, 3043–3047.
- Chan, D.C., 2006. Mitochondrial fusion and fission in mammals. *Annu. Rev. Cell Dev. Biol.* 22, 79–99.
- Cheung, E.C., McBride, H.M., Slack, R.S., 2007. Mitochondrial dynamics in the regulation of neuronal cell death. *Apoptosis* 12, 979–992.
- Chipuk, J.E., Green, D.R., 2008. How do BCL-2 proteins induce mitochondrial outer membrane permeabilization? *Trends Cell Biol.* 18, 157–164.
- Culmsee, C., Gerling, N., Landshamer, S., Rickerts, B., Duchstein, H.J., Umezawa, K., Klumpp, S., Kriegelstein, J., 2005a. Nitric oxide donors induce neurotrophin-like survival signaling and protect neurons against apoptosis. *Mol. Pharmacol.* 68, 1006–1017.
- Culmsee, C., Plesnila, N., 2006. Targeting Bid to prevent programmed cell death in neurons. *Biochem. Soc. Trans.* 34, 1334–1340.
- Culmsee, C., Zhu, C., Landshamer, S., Becattini, B., Wagner, E., Pellecchia, M., Blomgren, K., Plesnila, N., 2005b. Apoptosis-inducing factor triggered by poly(ADP-ribose) polymerase and Bid mediates neuronal cell death after oxygen–glucose deprivation and focal cerebral ischemia. *J. Neurosci.* 25, 10262–10272.
- Danial, N.N., Korsmeyer, S.J., 2004. Cell death: critical control points. *Cell* 116, 205–219.
- Desagher, S., Martinou, J.C., 2000. Mitochondria as the central control point of apoptosis. *Trends Cell Biol.* 10, 369–377.
- Duvezin-Caubet, S., Jagasia, R., Wagener, J., Hofmann, S., Trifunovic, A., Hansson, A., Chomyn, A., Bauer, M.F., Attardi, G., Larsson, N.G., Neupert, W., Reichert, A.S.,

2006. Proteolytic processing of OPA1 links mitochondrial dysfunction to alterations in mitochondrial morphology. *J. Biol. Chem.* 281, 37972–37979.
- Green, D.R., 2005. Apoptotic pathways: ten minutes to dead. *Cell* 121, 671–674.
- Ishihara, N., Jofuku, A., Eura, Y., Mihara, K., 2003. Regulation of mitochondrial morphology by membrane potential, and DRP1-dependent division and FZO1-dependent fusion reaction in mammalian cells. *Biochem. Biophys. Res. Commun.* 301, 891–898.
- Karbowska, M., Jeong, S.Y., Youle, R.J., 2004. Endophilin B1 is required for the maintenance of mitochondrial morphology. *J. Cell Biol.* 166, 1027–1039.
- Karbowska, M., Youle, R.J., 2003. Dynamics of mitochondrial morphology in healthy cells and during apoptosis. *Cell Death Differ.* 10, 870–880.
- Kazhdan, I., Long, L., Montellano, R., Cavazos, D.A., Marciniak, R.A., 2006. Targeted gene therapy for breast cancer with truncated Bid. *Cancer Gene Ther.* 13, 141–149.
- Kluck, R.M., Bossy-Wetzel, E., Green, D.R., Newmeyer, D.D., 1997. The release of cytochrome c from mitochondria: a primary site for Bcl-2 regulation of apoptosis. *Science* 275, 1132–1136.
- Knott, A.B., Bossy-Wetzel, E., 2008. Impairing the mitochondrial fission and fusion balance: a new mechanism of neurodegeneration. *Ann. NY Acad. Sci.* 1147, 283–292.
- Knott, A.B., Perkins, G., Schwarzenbacher, R., Bossy-Wetzel, E., 2008. Mitochondrial fragmentation in neurodegeneration. *Nat. Rev. Neurosci.* 9, 505–518.
- Kroemer, G., Galluzzi, L., Brenner, C., 2007. Mitochondrial membrane permeabilization in cell death. *Physiol. Rev.* 87, 99–163.
- Lackner, L.L., Nunnari, J.M., 2008. The molecular mechanism and cellular functions of mitochondrial division. *Biochim. Biophys. Acta.*
- Landshamer, S., Hoehn, M., Barth, N., Duvezin-Caubet, S., Schwake, G., Tobaben, S., Kazhdan, I., Becattini, B., Zahler, S., Vollmar, A., Pellicchia, M., Reichert, A., Plesnila, N., Wagner, E., Culmsee, C., 2008. Bid-induced release of AIF from mitochondria causes immediate neuronal cell death. *Cell Death Differ.* 15, 1553–1563.
- Liesa, M., Palacín, M., Zorzano, A., 2009. Mitochondrial dynamics in mammalian health and disease. *Physiol. Rev.* 89, 799–845.
- Liu, Y., Peterson, D.A., Kimura, H., Schubert, D., 1997. Mechanism of cellular 3-(4,5-dimethylthiazol-2-yl)-2,5-diphenyltetrazoliumbromide (MTT) reduction. *J. Neurochem.* 69, 581–593.
- Lovell, J.F., Billen, L.P., Bindner, S., Shamas-Din, A., Fradin, C., Leber, B., Andrews, D.W., 2008. Membrane binding by tBid initiates an ordered series of events culminating in membrane permeabilization by Bax. *Cell* 135, 1074–1084.
- Okamoto, K., Shaw, J.M., 2005. Mitochondrial morphology and dynamics in yeast and multicellular eukaryotes. *Annu. Rev. Genet.* 39, 503–536.
- Parone, P.A., Da, C.S., Tondera, D., Mattenberger, Y., James, D.I., Maechler, P., Barja, F., Martinou, J.C., 2008. Preventing mitochondrial fission impairs mitochondrial function and leads to loss of mitochondrial DNA. *PLoS ONE* 3, e3257.
- Plesnila, N., Zinkel, S., Le, D.A., min-Hanjani, S., Wu, Y., Qiu, J., Chiarugi, A., Thomas, S.S., Kohane, D.S., Korsmeyer, S.J., Moskowitz, M.A., 2001. BID mediates neuronal cell death after oxygen/glucose deprivation and focal cerebral ischemia. *Proc. Natl. Acad. Sci. USA* 98, 15318–15323.
- Rube, D.A., van der Blik, A.M., 2004. Mitochondrial morphology is dynamic and varied. *Mol. Cell. Biochem.*, 331–339.
- Santel, A., Frank, S., 2008. Shaping mitochondria: the complex posttranslational regulation of the mitochondrial fission protein DRP1. *IUBMB Life* 60, 448–455.
- Seiler, A., Schneider, M., Forster, H., Roth, S., Wirth, E.K., Culmsee, C., Plesnila, N., Kremmer, E., Radmark, O., Wurst, W., Bornkamm, G.W., Schweizer, U., Conrad, M., 2008. Glutathione peroxidase 4 senses and translates oxidative stress into 12/15-lipoxygenase dependent- and AIF-mediated cell death. *Cell Metab.* 8, 237–248.
- Suen, D.F., Norris, K.L., Youle, R.J., 2008. Mitochondrial dynamics and apoptosis. *Genes Dev.* 22, 1577–1590.
- Wang, X., 2001. The expanding role of mitochondria in apoptosis. *Genes Dev.* 15, 2922–2933.
- Wasiak, S., Zunino, R., McBride, H.M., 2007. Bax/Bak promote sumoylation of DRP1 and its stable association with mitochondria during apoptotic cell death. *J. Cell Biol.* 177, 439–450.
- Wasilewski, M., Scorrano, L., 2009. The changing shape of mitochondrial apoptosis. *Trends Endocrinol. Metab.* 20, 287–294.
- Youle, R.J., Karbowska, M., 2005. Mitochondrial fission in apoptosis. *Nat. Rev. Mol. Cell Biol.* 6, 657–663.
- Youle, R.J., Strasser, A., 2008. The BCL-2 protein family: opposing activities that mediate cell death. *Nat. Rev. Mol. Cell Biol.* 9, 47–59.